Roughness Measurements of Soil Surfaces by Acoustic Backscatter

Michael L. Oelze,* James M. Sabatier, and Richard Raspet

ABSTRACT

The measurement of the roughness of soil surfaces on centimeter scales is important to modeling local soil erodibility. An acoustic backscatter technique was examined for its ability to quantify the roughness of porous soil on centimeter scales. Acoustic backscatter offers the possibility of an inexpensive, mobile, and rapid means of estimating statistical properties of soil surfaces. Four soil plots were constructed with varying amounts of roughness. Surface roughness of the four soil plots was measured with the acoustic backscatter technique and a laser microreliefmeter. The roughness power spectra for the surface plots were obtained from surface profiles measured by the laser microreliefmeter and by the acoustic backscatter technique. Statistical values of the RMS (root mean square) height and correlation length of surface roughness for each plot were calculated from the acoustic backscatter power spectra and laser microreliefmeter power spectra and compared. Agreement between the two techniques for estimating roughness statistics was shown to be good (<13% difference) when an adequate amount of data points were used to map out the roughness power spectra. The acoustic backscatter technique appears to be a potential alternative to rapidly and inexpensively quantify the roughness of soil surfaces.

Quantitative descriptions of surface roughness are important in evaluating tillage and in simulating erosion processes. Few studies involving quantitative measures of surface roughness have been conducted. The major concern for describing a rough surface is constructing an adequate model to characterize the apparent random nature of surface roughness and then finding an adequate means of measuring model parameters.

Kuipers (1957) first introduced parameters that have been used in the past to describe surface roughness. Kuipers defined a roughness index $R_K = 100 \log(\sigma)$ in which σ is the standard deviation of the elevations readings of the surface. Following this, Allmaras et al. (1966) refined Kuipers roughness index by measuring the standard error of measured elevation points referenced to some plane. Several studies involving roughness characterization on surfaces used these parameters (Mitchell, 1970; Moore and Larson, 1979; Linden, 1979; Onstad, 1984).

A major critique with using the roughness index was that this roughness parameter did not describe the spatial dependence of the roughness elements. The roughness index characterized the variation of heights, or vertical roughness, but did not describe the spatial distribution of roughness on the surface. For example, two surfaces may have the same roughness index but one surface may have the roughness on average spaced farther apart on the surface. A more complete characterization would describe not only vertical scales of roughness but also the horizontal scales.

Römkens and Wang (1987) proposed two new parameters to describe both the roughness with elevation and the horizontal scale, or spatial dependency, of the roughness. One roughness parameter used to describe a transect of a rough surface was introduced by Römkens and Wang (1986a) as

$$R = A \times F \quad [1]$$

where A is the microrelief index (mm) and F is the peak frequency factor (mm^{-1}). A and F were used to describe the average-clod size and clod frequency, respectively. The microrelief index, A, is defined as the area per unit length between the measured surface profile and the regression line of least squares through all measured elevations on a transect.

The spatial distribution and the spatial dependence of the roughness were evaluated by the autocorrelation function, δ, of the roughness parameter, R, of successive transects. The correlation length for spatial independence was determined where the correlation function dropped to 0.2 of its initial value. A smaller spatial independence was found for surfaces that had been chiseled repeatedly as opposed to surface with little tillage (Römkens and Wang, 1987). The more a surface is chiseled the smaller the clod sizes. Smaller scaled roughness should tend to become uncorrelated at shorter lengths than larger scaled roughness.

Huang (1998) proposed an alternate description of surface roughness that would measure vertical and horizontal scales of roughness. The statistics by Huang (1998) utilized the fractal nature of random rough surfaces to describe the roughness. The fractal dimension, D, and the crossover length, l, were used to describe the semivariance function

$$\gamma(h) = 0.5E(|Z_x - Z_{x+h}|)^2 \quad [2]$$

where Z_x and Z_{x+h} are the roughness heights at positions separated by a horizontal distance h and E () is the expectation. The crossover length and fractal dimension described the relative magnitude and slope of the semivariance function, respectively. Huang and Bradford (1992) used the semivariance description to characterize roughness of soil plots as they changed because of rainfall.

Several instruments have been used in the past to obtain the surface roughness statistical characterizations from measured elevation data. Contact type microreliefmeters have been used to measure surface roughness

M.L. Oelze, Department of Electrical and Computer Engineering, University of Illinois, Urbana, IL 61801; and J.M. Sabatier and R. Raspet, National Center for Physical Acoustics, The University of Mississippi, Coliseum Drive, University, MS 38677. Received 9 July 2001. *Corresponding author (oelze@uiuc.edu).

Published in Soil Sci. Soc. Am. J. 67:241–250 (2003).

Abbreviations: RMS, root mean square.

(Radke et al., 1981; Podmore and Huggins, 1981). Contact methods tend to be time-consuming, cumbersome, and have the great disadvantage of disturbing or damaging the soil surface. Photogrammetry has been used to obtain elevation measurements from soil surfaces (Welch et al., 1984). Flanagan et al. (1995) noted that the photogrammetric method needed costly equipment for measurements and data processing and interpretation of the photogrammetric data is complicated. Römkens and Wang (1986b) first described the use of a noncontact-laser microreliefmeter at the Fourth Federal Interagency Sedimentation Conference. A subsequent paper (Römkens et al., 1988) described in detail the operation and performance of the laser microreliefmeter.

The laser microreliefmeter described by Römkens et al. (1988) could measure elevation data of rough soil surfaces without disturbing the soil surface. However, the equipment is expensive, somewhat bulky and scan times can take several hours for a plot of 60 by 60 cm. Flanagan et al. (1995) developed an automated laser scanner that kept an equivalent elevation resolution as the laser microreliefmeter but decreased the scan time. An alternate noncontact method was proposed by Oelze et al. (2001) using acoustic backscatter techniques to measure surface roughness statistics. The goal was to find a quick, mobile, and inexpensive means to evaluate surface roughness statistics.

Surface roughness characterization by the use of acoustic backscatter has been used for many years in the underwater acoustics community. A review of acoustic backscatter to characterize surface roughness in underwater sound is presented in Jackson et al. (1986). Use of an acoustic backscatter technique to measure surface roughness offers the possibility of an inexpensive and quick method of determining surface roughness statistics.

THEORY

Description of Acoustic Backscatter Theory

Acoustic backscatter from rough surfaces can be modeled using first-order perturbation theory at a rough fluid–fluid interface. First-order perturbation theory is valid under the constraints that (Ishimaru, 1978)

$$k_a h \sin\theta_g < 1/2 \qquad [3]$$

where h is the RMS height of the surface, k_a is the acoustic wavenumber, and θ_g is the graze angle. The acoustic wavenumber is inversely proportional to the wavelength of the sound propagating in air. The first-order backscatter cross section is given by

$$\sigma_p(\theta_g) = 4k_a^4 \sin^4\theta_g |Y(k_a, \theta_g)|^2 W(2k_a \cos\theta_g) \qquad [4]$$

where $W(2k_a \cos\theta_g)$ is the two-dimensional roughness power spectrum (Jackson et al., 1996) evaluated at the roughness wavenumber, $2k_a\cos\theta_g$. When the interface relief is small compared with wavelength, scattering comes from all points on the surface. Roughness elements with different separations or wavelengths between them will interfere differently back at the measurement transducer. The roughness wavenumber measured by the acoustic backscatter represents scattered wavelets coming from the surface that have the maximum constructive interference. The roughness wavenumber is inversely proportional to the wavelength of element separation where maximum constructive interference occurs. The power spectrum describes the amount of power scattered by a particular roughness wavenumber (roughness size). If more of a particular roughness size exists in an area analyzed by the sound wave then the scattered power corresponding to that roughness wavenumber will be greater.

The middle term of Eq. [4] is a modified reflection coefficient obtained by Kuo (1964),

$$Y(k_a, \theta_g) = \frac{(\rho - 1)^2 \cos^2\theta_g + \rho^2 - \kappa^2}{[\rho \sin\theta_g + \sqrt{\kappa^2 - \cos^2\theta_g}]^2} \qquad [5]$$

where ρ is the ratio of the bulk density of the surface material to the density of air and κ is the ratio of acoustic wavenumbers of the ground to acoustic wavenumbers of the air. Substituting the complex wavenumber and complex density from Attenborough's (1983) analysis of rigid frame porous materials yields the modified reflection coefficient in terms of the surface impedance

$$Y(k_a, \theta_g) = \frac{\left[Z - \frac{k_a}{k_b}\right]^2 \cos^2\theta_g + Z^2 - 1}{\left[Z \sin\theta_g + \sqrt{1 - \left(\frac{k_a \cos\theta_g}{k_b}\right)^2}\right]^2} \qquad [6]$$

where k_b is the complex wavenumber (acoustic wavenumber of the ground) of the porous soil surface, Z is the complex acoustic impedance of the soil surface.

The acoustic surface impedance and complex wavenumber describing a porous soil are functions of the frequency of sound and the pore properties of the soil surface. The acoustic impedance and complex wavenumber describe the interaction of sound with the soil. For large surface impedance the sound will be perfectly reflected from the surface. For a finite surface impedance the amount of sound absorbed by the surface will depend on the frequency of sound and pore properties of the soil. Numerous experiments have supported the impedance models describing the interaction of sound with porous materials (Sabatier et al., 1990; Attenborough, 1992; Fredrickson et al., 1996; Sabatier et al., 1996).

The pore properties that influence the propagation of sound into and through the soil are the porosity, tortuosity, and effective flow resistivity. The complex surface impedance is related to the pore properties by

$$Z = \frac{1}{\Omega\sqrt{\gamma}} \frac{\left[\frac{4}{3} T + i\left(\frac{4\sigma_{eff}}{2\pi f \rho_0}\right)\right]}{\left[aT + i\left(\frac{4\sigma_{eff}}{2\pi f \rho_0}\right)\right]^{1/2}} \qquad [7]$$

where Ω is the porosity, T is the tortuosity, σ_{eff} is the effective flow resistivity, γ is the ratio of specific heats for air, f is the acoustic frequency of operation, and a is constant equal to 1.106. The effective flow resistivity measures the permeability of the soil to sound. A high flow resistivity means that the surface becomes more impenetrable to sound or acoustically harder. The value of porosity is always <1, the tortuosity is typically <10 and the effective flow resistivity can range from 100 to 10×10^6 (kg m^{-2} s^{-1} or mks Rayls m^{-1}). For acoustically harder surfaces (effective flow resistivity $>3 \times 10^5$ kg m^{-2} s^{-1} [mks Rayls m^{-1}]) the impedance is dominated by the flow resistivity term and the other pore properties have negligible effect. Any arbitrary choice for the porosity and tortuosity will

have negligible effect on the modified reflection coefficient. Furthermore, the response of the complex surface impedance to changes in flow resistivity for acoustically harder surfaces is very small (Oelze, 2000).

For acoustically harder surfaces, such as rain sealed agricultural surfaces, assuming a value for the effective flow resistivity of 1×10^6 gives the magnitude of the modified reflection coefficient with minimal error. The contribution of the modified reflection coefficient to the acoustic backscatter measurement is calculated from the values of the complex surface impedance and wavenumber approximated from the assumed value of the effective flow resistivity and arbitrary values for the tortuosity and porosity. The two-dimensional roughness power spectrum can then be determined at a particular frequency and graze angle by relating an acoustic backscatter strength measurement, $S_s(k_a,\theta_g)$, with $10\log_{10}$ of the theoretical perturbation cross section, Eq. [4]

$$10\log_{10}W(2k_a\cos\theta_g) = S_s(k_a, \theta_g) - 10\log_{10}4k_a^4\sin^4\theta_g\,|Y(k_a, \theta_g)|^2. \quad [8]$$

By varying the frequency of operation and graze angle, different portions of the roughness power spectrum, $W(k_a, \theta_g)$, may be mapped out. If the effective flow resistivity is smaller than 3×10^5 kg m^{-2} s^{-1} (mks Rayls m^{-1}), additional measurements of the soil pore properties need to be made to extract the roughness properties from the backscatter measurement (Oelze et al., 2001).

Random or pseudorandom rough surfaces tend to have roughness power spectra that have power law dependence (Jackson et al., 1996). Soil plots broken up with farming implements were also shown to have power law dependence (Oelze et al., 2001). When plotting a power spectrum that is a power law in log-log space the power spectrum is a line. All that is needed to describe a line is two points, which means that relatively few measurements are needed to approximate the roughness power spectrum. The acoustic backscatter technique offers the ability to measure the roughness power spectrum quickly with a few measurements.

Proposal and Description of Surface Statistics

The acoustic backscatter technique measures the two-dimenstional power spectrum of the surface roughness profile. The power spectrum of a rough surface profile $z(x,y)$ is defined as

$$W(k_x, k_y) = |F\{z(x, y)\}|^2; \quad [9]$$

the magnitude squared of the Fourier transform of the height profile. The power spectrum is a convenient statistical description of a rough surface. The power spectrum is related to the semivariance function used by Huang (1998). Instead of describing the shape of the roughness power spectrum (or semivariance function) as Huang (1998), two independent parameters explicitly describing both horizontal and vertical scales of roughness were calculated from the roughness power spectrum. The RMS height, which describes the variation of heights about some mean height, can be found by the equation.

$$h_{RMS}^2 = 2\pi\int_{k_L}^{k_H} W(k)k\,dk. \quad [10]$$

Likewise, the autocorrelation function for the surface profile, $z(x,y)$, is given by

$$C(x) = \frac{2\pi}{h_{RMS}^2}\int_{k_L}^{k_H} W(k)\exp(-ikx)\,k\,dk \quad [11]$$

where k_L and k_H are the low and high cutoff wavenumbers respectively. The correlation length, L_c, is the length at which the correlation function drops to $1/e$ of its initial value. The correlation length value describes the spatial arrangement of roughness on the surface. A surface with roughness that changes rapidly, that is smaller clods, will have a shorter correlation length than a surface that has slow undulating roughness.

The low and high cutoff wavenumbers are important to the statistical description of the roughness. The low cutoff wavenumber, k_L, is chosen based on the size of the surface being measured. If the low wavenumber cutoff were chosen corresponding to a wavelength of several kilometers, then the roughness of larger scale valleys and hills would be added in the roughness calculation. Likewise, a high cutoff wavenumber, k_H, should also be chosen. A high cutoff wavenumber of infinity corresponds to adding atomic scale roughness into the roughness statistics calculation. The higher the value for the high cutoff wavenumber that is chosen, the smaller the roughness scales that will be included in the statistical calculations. Cutoff wavenumbers should be chosen with respect to the surface length being considered. For agricultural surfaces a low cutoff on the scale of meters should be chosen. In this work a low cutoff corresponding to 60 cm was chosen because it was the lengths of the transects measured by the laser microreliefmeter. The high cutoff wavenumber was chosen corresponding to 3 mm, the sampling grid of the laser microreliefmeter. All roughness statistics should be referenced to the cutoff wavenumbers used in calculation (Bennett and Mattson, 1989). The roughness wavenumbers used in this study ranged from a minimum of 10 m^{-1} to a maximum of 1000 m^{-1}.

A comparison of the roughness parameters, R and δ, used by Römkens and Wang (1986a) with the roughness statistics calculated from acoustic backscatter show that the two sets of statistics do not necessarily track the same changes in roughness. As an example, Fig. 1 shows a schematic of two hypothetical rough surfaces with different sizes and spatial spreading. The microrelief parameter and peak frequency remain the same for both surfaces while the RMS height increases for the second surface by a factor of $\sqrt{2}$ and the correlation length decreases slightly. The roughness parameter, R, does not show any difference between the two surfaces.

The more rapid the roughness changes over a certain length, the more quickly the surface would become uncorrelated with itself, that is, a shorter correlation length. The second surface

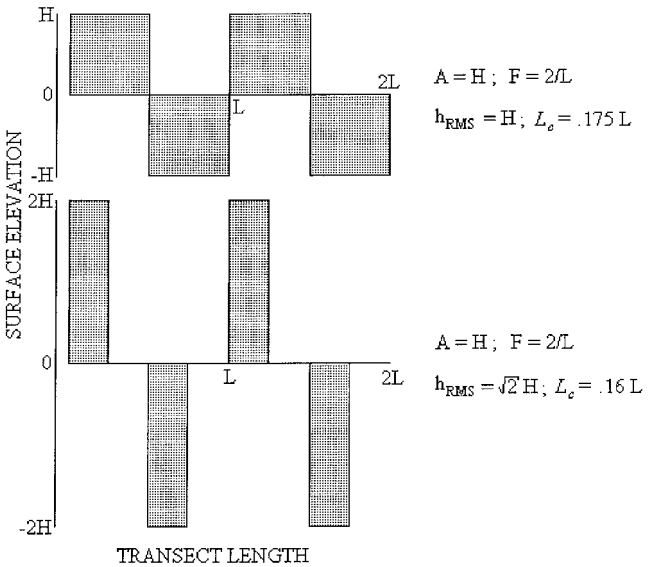

Fig. 1. Schematic representations of two hypothetical rough-surface transects with associated roughness statistics.

of Fig. 1 is changing more rapidly in spatial extent then the first surface, which is reflected by the decrease in correlation length for the second surface. Likewise, if the surface is changing rapidly with spatial extent the spatial independence parameter, δ, would be expected to be smaller. There is not a one to one correlation between the spatial independence parameter and the correlation length statistic but both quantify spatial arrangement of surface roughness.

MATERIALS AND METHODS

Plot Preparation

Four soil plots were constructed with different roughness sizes to determine the ability of acoustic backscatter to differentiate roughness sizes. Each plot size was 1.5 by 12 m. The four surfaces were constructed by using farm and gardening implements to break up the soil into smaller and smaller clods. The plots were made with different sized roughness. Clods were broken up on the surface with a hoe and then broken down further with a metal rake.

The first three surfaces were coated with dissolved Saran powder (DOW Chemical Co.,). Typical agricultural fields sealed by rainfall have a large flow resistivity or low acoustic permeability (Attenborough, 1992). A surface with a large flow resistivity ($>10^7$ kg m^{-2} s^{-1} [mks Rayls m^{-1}]) is nearly impermeable to sound. The Saran coating acted to decrease the acoustic permeability of the surface to that of typical agricultural surfaces sealed by a rainfall. By coating the surface with the dissolved Saran powder, the changes to the roughness were minimized. After the plots were constructed they were covered with shelters to prevent further weathering and minimize surface evolution.

The fourth plot was not coated with dissolved Saran powder but was left open to a rainstorm. The rain acted to further change the roughness of the soil plot and decreased the acoustic permeability of the surface. The fourth plot was then covered with a shelter to prevent further weathering and minimize surface erosion.

Description of the Laser Microreliefmeter Measurements

The laser microreliefmeter was used to measure the roughness of the four rough soil plots. The roughness statistics estimated from the laser microreliefmeter were used as a comparison to verify the acoustic backscatter statistical estimates. Transects of 60 cm in length were measured from the surface in the horizontal direction perpendicular to the tracks (*x*-direction). Each transect was taken by recording the laser microreliefmeter readings at certain time intervals as the motor translated the profiler in the *x*-direction. A computer program that read in the values obtained by the laser microreliefmeter controlled the motor. The spacing between each point was determined by the speed of the motor, that is the slower the motor the more points that were obtained over a certain distance. The sampling length in the *x*-direction was found by dividing the total sampled length by the number of points per transect. The average sampling length was found to be around 2.7 mm in the *x*-direction. After a transect was measured in the *x*-direction, the laser microreliefmeter was translated along the *y*-direction by 3 mm and another transect was measured. The process was repeated until 200 transects were taken to measure an area of approximately 60 by 60 cm. After measuring each transect, a matrix of $\mathbf{N_x} \times \mathbf{N_y}$ height values was obtained. This matrix or area profile, **z(x,y)**, could be broken into separate *x* and *y* transects.

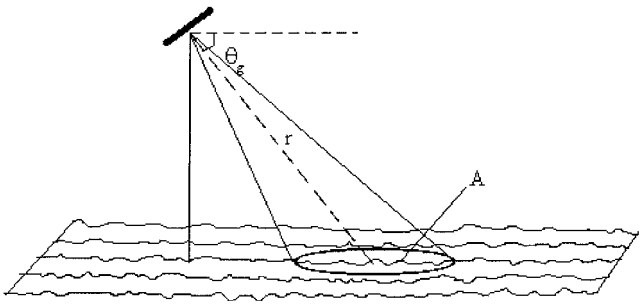

Fig. 2. Typical backscatter experimental setup with graze angle, θ_g, distance on transducer axis from transducer to surface, *r*, and area of ensonified surface, *A*.

While an area was measured with the laser microreliefmeter, the average one-dimensional power spectrum was calculated by averaging the one-dimensional power spectra from transects recorded in the *x* and *y* directions. Averaging allowed for the power spectrum to be smoothed and to decrease the effects of anomalous roughness. From a height profile transect, the one-dimensional power spectrum was calculated through the equation:

$$W(k) = \frac{1}{2\pi L}\left|\int_0^L z(x)\exp(ikx)\mathrm{d}x\right|^2 \qquad [12]$$

where *L* is the length of the transect. If the surface is assumed to be isotropic in both *x*- and *y*-directions then the two-dimensional roughness power spectrum of the surface area could be calculated from the average one-dimensional power spectrum (Jackson and Briggs, 1992). The two-dimensional roughness power spectrum calculated from the average one-dimensional roughness power spectrum was smoother than the two-dimensional roughness spectrum calculated from the area height profile. The smoothing of the one-dimensional roughness power spectrum was a result of the averaging of the individual one-dimensional roughness power spectra from each transect.

Description of the Acoustic Backscatter Measurements

Acoustic backscatter techniques relate measurements of the intensity of backscattered sound from a rough surface to models describing the surface properties. Figure 2 shows a typical setup for an acoustic backscatter measurement from a rough surface. A transducer is positioned at some height above a rough surface pointed at some angle, θ_g, toward the surface. The graze angle, θ_g, is measured from a plane parallel to the surface. Sound is emitted from the transducer toward the surface in the form of a pulse or tone burst. The transducer is operated in pulse/echo mode so that it is used not only as the transmitter but also as the receiver. The sound that scatters back toward the transducer is called the backscatter. When the size of the transducer aperture is larger than the wavelength of sound, the sound emitted is in an acoustic beam. A beam enables the sound to be directed to a specific spot on the surface. In Fig. 2, *A* represents the area ensonified by the acoustic beam.

Acoustic backscatter is measured in terms of the scatter strength, with units in decibels (dB). The backscatter strength is defined as

$$S_s = 10\log_{10}(\sigma) \qquad [13]$$

where σ is the backscattered cross section defined as

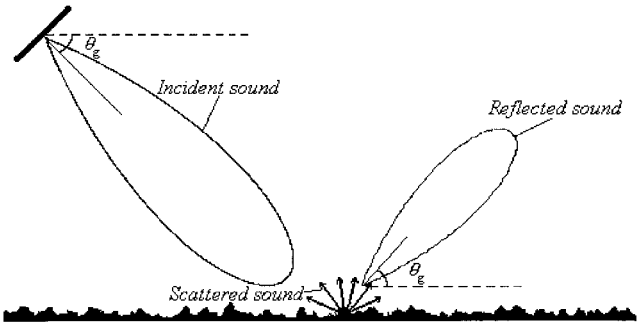

Fig. 3. Reflection and scattering of incident sound from a rough surface.

$$\sigma = \frac{r^2}{A}\frac{I_s}{I_0} \qquad [14]$$

where I_s is the intensity of the field scattered back toward the source, r is the distance from the source to the ensonified area, I_0 is the incident intensity, and A is the area of the ensonified patch. The scattered intensities are measured and inserted in Eq. [14] to calculate the backscatter cross section. The effect of the equipment on the scattered returns is taken out by the substitution method (Sigelmann and Reid, 1973). The same transducer used in the scattering experiment is used to measure the reflection of the pulse from a planar surface at normal incidence. The planar surface in this work was a large sheet of plexiglass that was assumed to be a perfect reflector. The reflected pulse is used as a reference for the incident pulse. Since the same equipment and settings were used for the incident and scattered intensities, the effect of the equipment on the measured cross section is canceled out.

When sound is incident on a rough soil surface with graze angle, θ_g, most of the sound is reflected away from the transducer at an angle, θ_g. As shown in Fig. 3, a small portion of the sound is scattered from the roughness in all directions. The sound intensity level of the source must be large enough so that the portion of sound scattered from the surface is detectable above the noise. The sound intensity level (SIL) is a decibel scale and is defined as

$$\text{SIL} = 20 \log_{10} \frac{I_{ss}}{I_{ref}} \qquad [15]$$

where I_{ss} is the intensity of the sound source at 1 m and I_{ref} is a reference intensity for sound in air equal to 10^{-12} W m^{-2}. Since the scattering returns are usually on the order of 20 to 30 dB less than the incident sound level, it is necessary to have a source level at least 40 dB above the noise at the surface. Noise levels of sound outdoors are typically between 50 and 70 dB for the frequency ranges of 1 to 10 kHz. The source levels of transducers used for roughness characterization of porous soils outdoors should be at a minimum of 100 dB.

In the acoustic backscatter measurements taken on the four roughness plots a capacitor style transducer with grooved back plate covered by Mylar film was used (Shields et al., 1977). The transducer was circular with a diameter of around 25 cm and a flat frequency response over the ranges of 2.5 to 7 kHz. The height of the transducer was measured using a meter stick and the angle of grazing was measured with an inclinometer. The transducer was used in pulse/echo mode through a diode clamp over the frequency ranges of 1.5 to 10 kHz. Two or three cycles tone bursts were generated by an HP model 3314A function generator (Hewlett Packard, Palo Alto, CA) and amplified to the desired voltage (100–150 Vp-p) by means of

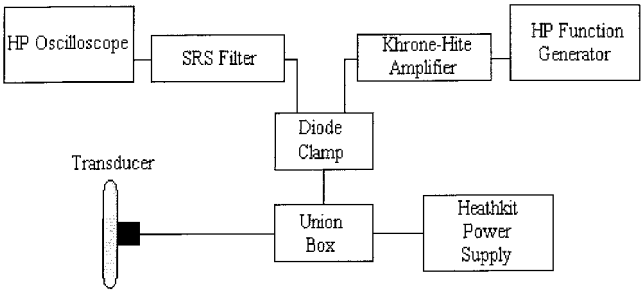

Fig. 4. Block diagram of the acoustic backscatter equipment.

a Krohn-Hite amplifier (Krohn-Hite Corp., Avon, MA). A 200-V DC bias was placed on the transducer using a Heathkit model IP-2717A power supply (Heath Co., Benton Harbor, MI). The AC and DC signals were combined in a union box circuit that blocked the DC voltage from going to the filter and oscilloscope. Backscatter signals were received by the same transducer and filtered and amplified by an SRS 650 filter (Stanford Research Systems, Sunnyvale, CA). The resulting signals were displayed on a HP model 54540C oscilloscope (Hewlett Packard, Palo Alto, CA) and saved to a disk for postprocessing. Figure 4 shows a diagram of the acoustic backscatter electronics and equipment. The price of the acoustic backscatter setup can be inexpensive. The device could be operated with a portable computer, A/D card, pulse-echo circuit, transducer, amplifier, and software for under $4500.

The scattered intensity was calculated by integrating the received backscattered echoes gated from the radio frequency (RF time signal corresponding to the surface area ensonified by sound. The area ensonified by sound was calculated from the beamwidth (−3 dB), the graze angle and the height of the transducer above the ground. The roughness wavenumber was calculated from the acoustic wavenumber and graze angle according to Eq. [4]. Equation [8] was then used to obtain the point on the roughness power spectrum corresponding to the roughness wavenumber. The value of the modified reflection coefficient in Eq. [8] was calculated by assuming a value of 1×10^6 kg m^{-2} s^{-1} (mks Rayls m^{-1}) for the effective flow resistivity. The choice of other pore property values was arbitrary.

The measurements were taken in the morning or in the night so that temperature gradients in the air above the soil would not be present. The temperature gradients above the soil surface are caused by the heating of the soil surface by the sun. The temperature of the soil surface and the air above it will be different as the soil absorbs heat from the sun. The temperature difference sets up a gradient that causes the speed of sound to change slightly over the temperature gradient. The changing speed of sound causes refraction of the acoustic waves. The refraction of the acoustic waves means that the angle of grazing is changed from what was measured. Wind did not have an appreciable effect on the acoustic measurements. However, care was taken to obtain measurements when the wind was not substantial.

For the measurements, the transducer was mounted to a movable cart. The mounting bar could be adjusted to change the elevation of the transducer element with respect to the surface. The elevation was chosen so that the footprint of the ensonified ground would be large enough to encompass the roughness wavenumber (wavelength) being examined. If the footprint of the ensonified ground were too small, measurements of power spectrum at the interrogated roughness wavenumber would be incorrect. The screw attaching the transducer to the mounting bar could adjust the graze angle of the transducer. The cart was manually rolled down the length of

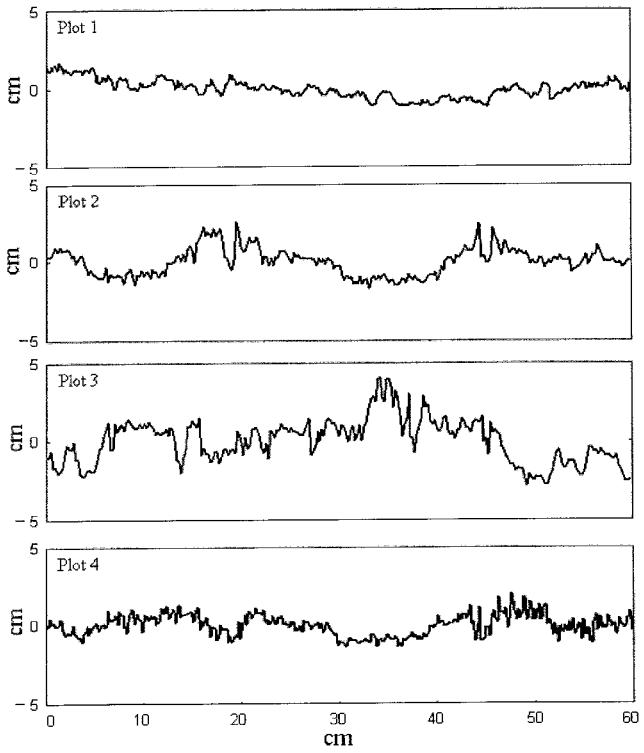

Fig. 5. Random transects of the four rough soil plots measured by the laser microreliefmeter.

a soil plot allowing measurements to be taken at different points on the surface for averaging. A scan of 30 points of the surface for a particular frequency and graze angle took approximately 15 min. The process could be automated to speed up scan times significantly.

RESULTS

Figure 5 shows random one-dimensional transects taken by the laser microreliefmeter of the four soil plots. The difference in the sizes of roughness are evident in the first three soil profiles with the largest being Plot 3 and smallest being Plot 1. Visual inspection of Plot 3 showed the largest roughness clod was on the order of 8 to 10 cm.

The roughness power spectra of the four soil plots were calculated from measurements by the acoustic backscatter technique and laser microreliefmeter. Acoustic backscatter measurements were taken at graze angles between 30° and 70° and at frequencies between 2.5 and 7 kHz. Assuming the surfaces were acoustically harder, the two-dimensional roughness power spectrum for each surface was determined for a particular frequency and graze angle according to Eq. [4]. By taking measurements at various frequencies and graze angles, different portions of the two-dimensional power spectrum were mapped out. Figure 6 shows the inverted acoustic data superimposed upon the two-dimensional power spectra measured by the laser microreliefmeter for the first three soil plots. The total length of the error bars on the acoustic data points represent one standard deviation about the mean value of 15 acoustic measurements taken at different points on the soil surface for each frequency and graze angle used. The laser microreliefmeter appeared to show a distinct difference between the three different roughness sized plots. The distinction between the smallest two roughness plots was not as clear from the acoustic data. The lack of distinction may have been a result of too few data points mapping out the roughness power spectra measured for the plots. Figure 7 shows the power spectra of the fourth soil plot calculated from the acoustic backscatter and laser microreliefmeter measurements. The data points represented an average of 30 measurements taken at a particular roughness wavenumber from different points on the surface. The error bars represented one full standard deviation about the average value of 30 measurements.

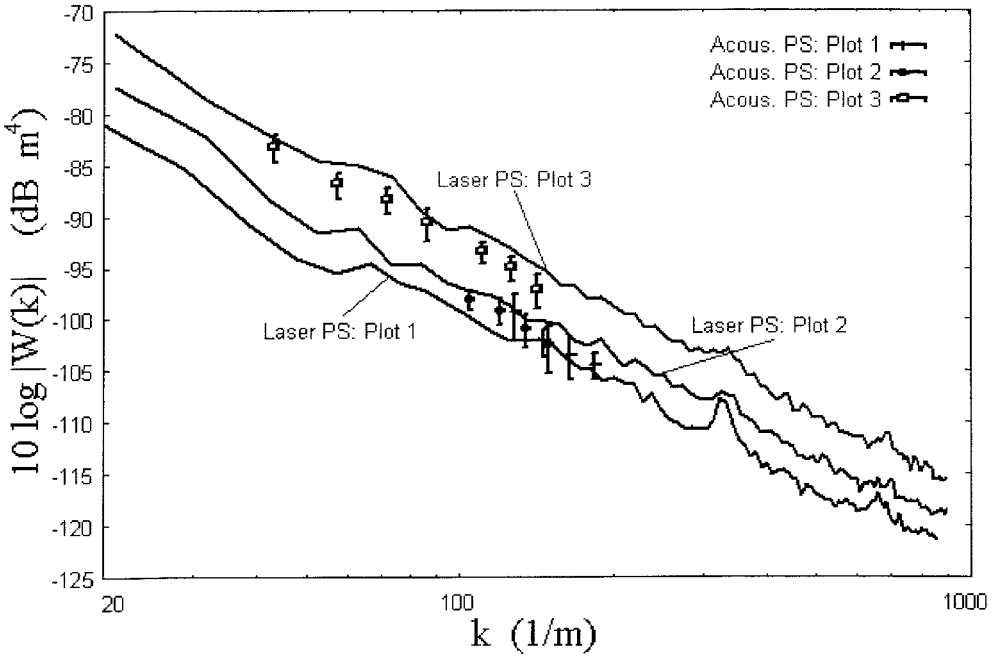

Fig. 6. Two-dimensional roughness power spectra of first three soil plots derived from measurements by acoustic backscatter and the laser microreliefmeter.

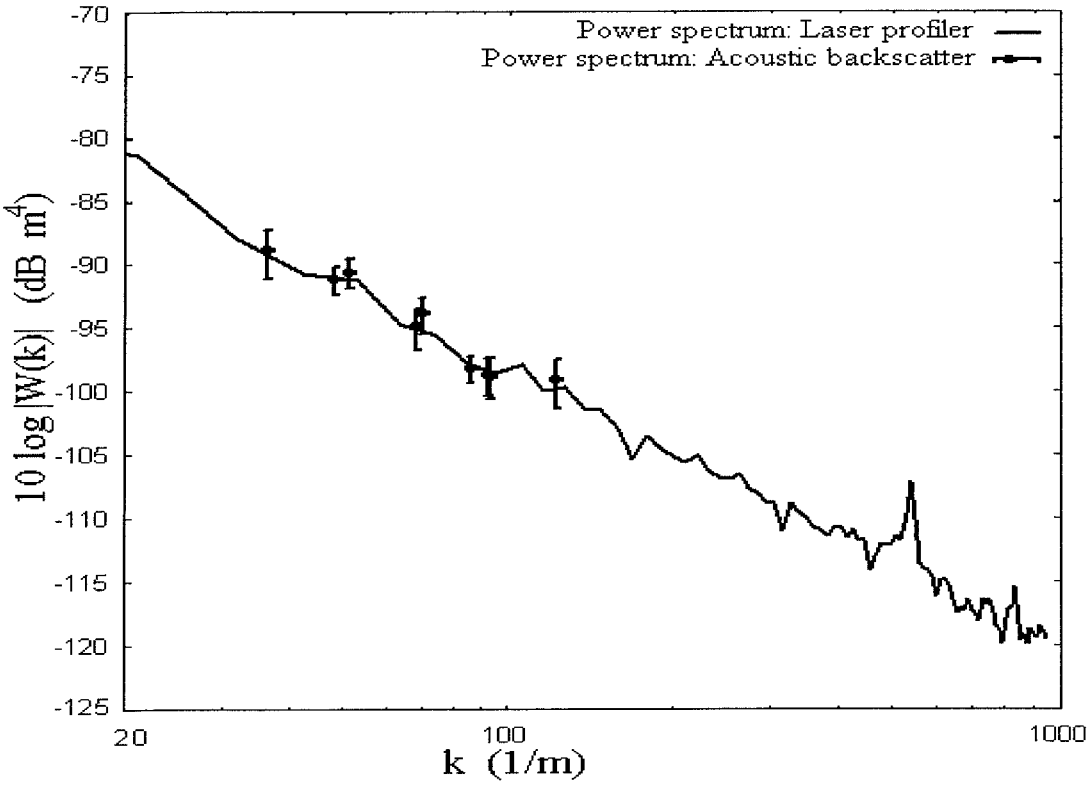

Fig. 7. Two-dimensional roughness power spectra of plot left open to rainfall derived from measurements by the acoustic backscatter and the laser microreliefmeter.

A best-fit line through each power spectrum in log-log space measured by the laser microreliefmeter and acoustic backscatter technique was calculated with least squares. Slopes and intercepts were also calculated from the best-fit lines. Table 1 lists the average of the slopes and intercepts calculated for the acoustic data and the least squares slope and intercept from the laser microreliefmeter power spectra. For the acoustic data, the best-fit line was calculated using the average points, the standard deviation for each point was not included in the regression analysis. The standard errors (Ott, 1993) for the slope and intercept parameters are included in Table 1 below each slope and intercept value. Examination of the different values in Table 1 shows the laser microreliefmeter data is within the standard error of the acoustic data.

From the values for the slope and intercept of the acoustic and laser data, values for the RMS height and the correlation function were determined. Using the functional form of the power law, the two-dimensional roughness power spectrum in polar coordinates is

$$W(k) = \beta \mathbf{k}^{-\gamma} \qquad [16]$$

where **k** represents the magnitude of the two-dimensional wave vector **k**. The slope (m) and intercept (b) of the roughness power spectrum in log-log space can be related to β and γ by

$$b = 10\log\beta \text{ and } m = -\gamma. \qquad [17]$$

Inserting Eq. [16] into Eq. [10] and [11] yields (Jackson et al., 1986)

$$h_{\mathrm{RMS}}^2 = \frac{2\pi\beta}{\gamma - 2}\left(k_{\mathrm{L}}^{-\gamma+2} - k_{\mathrm{H}}^{-\gamma+2}\right) \qquad [18]$$

and

$$C(x) = \frac{2\pi}{h_{\mathrm{RMS}}^2}\int_{k_{\mathrm{L}}}^{k_{\mathrm{H}}} \beta k^{-\gamma+1}\exp -ikx \, \mathrm{d}k. \qquad [19]$$

The integral for the correlation function is evaluated numerically. Equations [18] and [19] show the importance of the cutoff wavenumber choices to the values obtained for the RMS height and correlation length.

Table 1. Slopes and intercepts of best-fit lines to the two-dimensional power spectrums from both laser microreliefmeter and acoustic backscatter including standard errors.

	Slope			Intercept		
	Laser	Acoustic	% Diff.†	Laser	Acoustic	% Diff.
			Soil plots coated by Saran powder dissolved in MEK‡			
Plot 1	−2.41 ± .027	−2.29 ± .065	5.0	−51.2 ± .69	−52.7 ± 1.43	2.9
Plot 2	−2.42 ± .019	−2.10 ± .44	13.2	−48.0 ± .495	−56.0 ± 9.16	16.7
Plot 3	−2.58 ± .017	−2.58 ± .104	0.0	−39.7 ± .45	−40.6 ± 2.02	2.3
Plot 4	−2.20 ± .039	−2.25 ± .245	2.3	−54.4 ± .88	−53.2 ± 4.48	2.2

† Difference percentage.
‡ MEK, methylethyl ketone.

Table 2. Root mean square (RMS) height and correlation (Corr.) length calculated from the best-fit lines to the two-dimensional power spectra along with the percentage difference between the laser microreliefmeter and acoustic backscatter results.

	RMS height from best-fit line			Corr. length from best-fit line		
	Laser	Acoustic	% Diff	Laser	Acoustic	% Diff
Soil plots coated with dissolved Saran powder						
Plot 1	6.34 mm	6.85 mm	8.0	4.1 cm	3.2 cm	22
Plot 2	8.98 mm	7.2 mm	19.8	4.3 cm	1.8 cm	58
Plot 3	1.70 cm	1.55 cm	8.8	5.4 cm	5.4 cm	0.0
Soil plot exposed to rainfall						
Plot 4	6.88 mm	7.06 mm	2.6	2.6 cm	2.9 cm	12

The best-fit line represents an ensemble of averages of the power spectrum at many different spots on the surface. Suppose the roughness parameters were being measured for a large agricultural surface, the power spectrum obtained from one section of the surface will be slightly different from another section of the surface. A best-fit line represents an average of a large ensemble of power spectra from different sections. Calculating the RMS height and correlation length from the best-fit line gives the best representation of the statistics of the overall surface.

Table 2 shows the RMS height and correlation length values obtained from the slopes and intercepts in Table 1. The difference percentage between the acoustic and laser microreliefmeter data was calculated for the RMS height and correlation length. The difference in roughness sizes (RMS height) averaged from the laser microreliefmeter and acoustic backscatter estimates was statistically significant between Plots 1 and 3 and Plots 2 and 3 ($P < .05$). The difference between roughness sizes of Plots 1 and 2 was found not to be statistically significant ($P = .248$). The different sizes of roughness are also seen in the calculation of RMS height and correlation length for each surface.

From Fig. 6 and 7 it is seen that more acoustic data (more points mapped out on the roughness power spectrum) were compiled for Plot 4 and the largest roughness sized plot (Plot 3) than for the two smaller roughness plots. Tables 1 and 2 imply that calculating the slope and intercept from a few points as opposed to many reduces the accuracy of the overall results. Calculation of the correlation length seems to be particularly sensitive to the number of data points used to approximate the power spectrum.

The difference percentage between the laser profile data and acoustic data for values of slope and intercept ranged from 0.0 to 16.7. The smallest error came from Plot 3 where more data points than Plots 1 and 2 were measured allowing better averaging of results. Calculations of RMS height and correlation length from slopes and intercepts yielded even larger difference percentage. The percentage of difference in the RMS height ranged from 2.6 to 19.8 between the laser microreliefmeter and acoustic backscatter estimates. The smallest difference percentage came from the rainfall plot (Plot 4) that had the most overall acoustic data points measured on the roughness power spectrum. The measurement of the correlation length appeared to be more sensitive overall to measurement error. The maximum difference percentage came from Plot 2 with a 53.9% difference and the minimum error was from Plot 3 with a 0.0% difference. The theory used to obtain the roughness statistics was the perturbation approximation that assumed small roughness elements compared with acoustic wavelength. Since Plots 1 and 2 had smaller roughness than Plot 3, backscatter measurements should lead to better statistical approximations for Plots 1 and 2. The fact that Plot 2 yielded much worse results than Plot 3 stems from the fact that twice as many data points were obtained for Plot 3 allowing for a better linear fit to the data. In the case of Plot 1 the agreement was not nearly as bad as for Plot 2. Good linear fits may be made with just a few points but the possibility of making bad fits increased with fewer data points.

Differences in the best-fit line approximations could also be because of the different roughness wavenumber ranges used to make the fits. The laser microreliefmeter power spectrum was mapped out to roughness wavenumbers as large as 1000 m^{-1}. If the power law assumption did not hold over the full wavenumber range examined, disparities between the acoustic estimates and the laser microreliefmeter estimates would occur. If the agreement between linear parameters from the acoustic backscatter and laser microreliefmeter data was good, the power law assumption was assumed to be valid. The data showed that the power law assumption for the power spectrum described the surfaces well.

Comparisons of Table 1 and Table 2 showed that better results were obtained by taking more acoustic data points. The greatest difference between the acoustic and laser microreliefmeter roughness statistics came from Plot 2. The best-fit slope and intercept for Plot 2 also differed the most between acoustic and laser microreliefmeter values. The best agreement between the acoustic and the laser microreliefmeter slope and intercept values came from Plot 3 and 4. Error from the best-fit line propagated through to the calculation of roughness statistics, a large discrepancy between the slope and intercept values led to large differences in the RMS height and correlation length. The calculation of the correlation length appeared to be especially sensitive to values of slope and intercept. Analysis of the present data indicated that many points (7 or more) should be used to map out the roughness power spectrum to reduce error for the statistical calculations.

The acoustic backscatter technique was shown capable of giving estimates of the RMS height and correlation length of rough porous soil surfaces. The roughness could be separated from the effects of surface impedance for typical weathered agricultural surfaces. Typical weathered agricultural surfaces are surfaces that are acoustically harder. Acoustically harder surfaces were defined in this work as surfaces with effective flow resistivities of 3×10^5 kg m^{-2} s^{-1} (mks Rayls m^{-1}) and above. Values of flow resistivity for the experimental soil surfaces were measured by a Leonard's (1946) apparatus and found to range from 2×10^6 to 9×10^6 kg m^{-2} s^{-1} (mks Rayls m^{-1}).

For acoustically softer surfaces, that is those with flow

resistivities lower than 3×10^5 kg m^{-2} s^{-1} (mks Rayls m^{-1}), both the effects of the surface impedance and complex wavenumber must be measured. The effects of the surface impedance could be incorporated in the acoustic backscatter calculation by independent probe microphone measurements (Sabatier et al., 1990). For acoustically harder surfaces an independent measurement of the pore properties by the probe microphone is not needed. The effects of the surface impedance for acoustically harder surfaces could be assumed with a minimum of error.

The rough surface plots constructed for this study were made to have random roughness without ripples or tillage lanes. The assumption of isotropy was consistent with the construction of the four surface plots. The effects of tillage and regular ripples on the roughness would break the assumption of isotropy and clearly be seen by the laser microreliefmeter. Evidence exists (Jackson and Briggs, 1992) that the acoustic backscatter measurements may not be sensitive to surface anisotropy. Further study is needed to determine if acoustic backscatter can quantify the presence of directional ripples or other anisotropic roughness effects.

DISCUSSION

Roughness statistics estimated using laser microreliefmeter measurements and an acoustic backscatter technique were shown to be in good agreement when the number of acoustic measurements of the roughness power spectrum were adequate (7 or more). Roughness power spectra were calculated from both the laser microreliefmeter and acoustic backscatter data. From the acoustic backscatter data and laser microreliefmeter data the slope and the intercept could be calculated to approximate the roughness power spectrum in log-log space. Theoretically, only two data points were needed to obtain both the slope and intercept of the line approximating the power spectrum. As was expected, the results of the experiments showed that the more data points that were used to find the slope and intercept the better the lines approximating the roughness power spectra. Roughness statistics obtained from Plots 3 and 4 with the most acoustic data points gave the best overall agreement with the laser microreliefmeter results, less than 13% difference for both RMS height and correlation length.

The advantages to using the acoustic backscatter technique were several. The acoustic backscatter technique could more quickly measure the surface roughness statistics than the laser microreliefmeter, that is an hour as opposed to several hours. The acoustic backscatter device could be inexpensive to build. The acoustic backscatter device was also less bulky and more mobile than the existing laser microreliefmeter. A single person could setup and takedown the acoustic backscatter device. Several people were needed to setup and take down the laser microreliefmeter device at each run.

Some of the disadvantages of the acoustic backscatter device were its limitations. The acoustic backscatter device did not measure the full profile of a surface but gave only the surface statistics. Therefore, the laser microreliefmeter gave much more information about a surface and was useful over a broader range of applications. Also, the acoustic backscatter technique relied on relating scattered sound to perturbation theory. If the wavelength of sound was not large enough relative to the roughness, the theory would begin to break down. Likewise, if the surface was too acoustically soft, extra measurements of the pore properties would need to be made to accurately extract the roughness statistics from the backscatter measurements.

The results from the four roughness plots showed that the acoustic backscatter technique was feasible for measuring the roughness of porous soil. The utility of the acoustic backscatter technique could be increased by mapping out a larger range of roughness wavenumber values on the roughness power spectrum. Furthermore, to expand the capabilities of the acoustic backscatter technique, experiments need to be done on surfaces that are acoustically softer. Future directions for this work will include automating the process for more rapid measurements of acoustic backscatter data.

CONCLUSION

The acoustic backscatter technique was shown to give similar estimates of roughness statistics as the laser microreliefmeter. When an adequate amount of roughness wavenumbers were measured by the acoustic backscatter technique (Plots 3 and 4), differences between the laser microreliefmeter and acoustic backscatter were $<9\%$ for the RMS height estimates and $<13\%$ for the correlation length estimates. When just a few points on the roughness power spectra were measured by the acoustic backscatter technique, the differences between estimates made by the laser microreliefmeter and acoustic backscatter were worse (as large as 58% for correlation length estimate on Plot 2). The acoustic backscatter technique could provide accurate roughness statistics about soil surfaces in an inexpensive and efficient manner if an adequate number of points (7 or more) on the roughness power spectrum were measured.

ACKNOWLEDGMENTS

The authors thank the USDA for their entire support during this project. We thank Dr. M. J. M. Römkens for his helpful discussions and assistance in using the laser microreliefmeter, Dr. Craig Hickey and Dr. Jim Chambers for their discussions about this work and J. Y. Wang for her help in taking laser microreliefmeter measurements of rough surfaces.

REFERENCES

Allmaras, R.R., R.E. Burwell, W.E. Larson, and R.F. Holt. 1966. Total porosity and random roughness of the interrow zone as influenced by tillage. USDA Conserv. Res. Report No. 7. USDA-ARS, Washington, DC.

Attenborough, K. 1983. Acoustical characteristics of rigid fibrous absorbent and granular Materials. J. Acoust. Soc. Am. 73:785–799.

Attenborough, K. 1992. Ground parameter information for propagation modeling. J. Acoust. Soc. Am. 92:418–427.

Bennett, J.M., and L. Mattson. 1989. Introduction to Surface Roughness and Scattering. Opt. Soc. Am., Washington D.C.

Flanagan, D.C., C. Huang, L.D. Norton, and S.C. Parker. 1995. Laser scanner for erosion plot measurements. Trans. ASAE 38:703–710.
Fredrickson, C.K., J.M. Sabatier, and R. Raspet. 1996. Acoustic characterization of rigid-frame air-filled porous media using both reflection and transmission measurements. J. Acoust. Soc. Am. 99:1326–1332.
Huang, C., and J.M. Bradford. 1992. Application of a laser scanner to quantify soil microtopography. Soil Sci. Soc. Am. J. 56:14–21.
Huang, C. 1998. Quantification of surface microtopography and surface roughness. p. 153–168. *In* Baveye, Phillipe (ed.) Fractals in soil science. CRC Press, Boca Raton, FL.
Ishimaru, A. 1978. Wave Propagation and Scattering in Random Media, Vol. 2, Academic Press, Inc., New York.
Jackson, D.R., D.P. Winebrenner, and A. Ishimaru. 1986. Application of the composite roughness model to high-frequency bottom backscattering. J. Acoust. Soc. Am. 79:1410–1422.
Jackson, D.R., and K.B. Briggs. 1992. High-frequency bottom backscattering: Roughness versus sediment volume scattering. J. Acoust. Soc. Am. 92:962–977.
Jackson, D.R., K.B. Briggs, K.L. Williams, and M.D. Richardson. 1996. Test of models for high-frequency seafloor backscatter. IEEE J. Oceanic Eng. 21:458–470.
Kuipers, H. 1957. A relief meter for soil cultivation studies. Neth. J. Agric. Sci. 5:255–262.
Kuo, E.Y.T. 1964. Wave scattering and transmission on at irregular surfaces. J. Acoust. Soc. Am. 36:2135–2142.
Leonard, R.W. 1946. Simplified flow resistance measurements. J. Acoust. Soc. Am. 17:240–241.
Linden, D.R. 1979. A model to predict soil water storage as affected by tillage practices. Ph.D. thesis, University of Minnesota, St. Paul, MN.
Mitchell, J.K. 1970. Micro-relief depression storage. Ph.D. thesis, University of Illinois, Champaign, IL.
Moore, I.D., and C.L. Larson. 1979. Estimating microrelief surface storage from point data. Trans. ASAE 22:1073–1077.
Oelze, M.L., J.M. Sabatier, and R. Raspet. 2001. Roughness characterization of porous soil with acoustic backscatter. J. Acoust. Soc. Am. 109:1826–1832.
Oelze, M.L. 2000. Roughness characterization of porous soil using acoustic backscatter. Ph.D. thesis, University of Mississippi, MS.
Onstad, C.A. 1984. Depressional storage on tilled soil surfaces. Trans. ASAE 27:729–732.
Ott, R.L. 1993. An Introduction to Statistical Methods and Data Analysis. Marion Merrell Dow, Inc., Belmont, CA.
Podmore, T.H., and L.F. Huggins. 1981. An automated profile meter for surface roughness measurements. Trans. ASAE 24:663–665, 669.
Radke, J.K., M.A. Otterby, R.A. Young, and C.A. Onstad. 1981. A microprocessor automated rillmeter. Trans. ASAE 24:401–404, 408.
Römkens, M.J.M., and J.Y. Wang. 1986a. Effect of tillage on surface roughness. Trans. ASAE 29:429–433.
Römkens, M.J.M., and J.Y. Wang. 1986b. Sediment redistribution by raindrop impact. Proceedings of the Fourth Federal Interagency Sedimentation Conference, Las Vegas NV 1:10–17.
Römkens, M.J.M., and J.Y. Wang. 1987. Soil roughness changes from rainfall. Trans. ASAE 30:101–107.
Römkens, M.J.M., J.Y. Wang, and R.W. Darden. 1988. A laser microreliefmeter. Trans. ASAE 31:408–413.
Sabatier, J.M., H. Hess, W.P. Arnott, K. Attenborough, and M.J.M. Römkens. 1990. *In* situ measurements of soil physical properties by acoustical techniques. Soil Sci. Soc. Am. J. 54:658–672.
Sabatier, J.M., D.C. Sokol, C.K. Fredrickson, M.J.M. Römkens, E.H. Grissinger, and J.C. Shipps. 1996. Probe microphone instrumentation for determining soil physical properties: testing in model porous materials. Soil Technol. 8:259–274.
Shields, F.D., H.E. Bass, and L.N. Bolen. 1977. Tube method of sound-absorption measurement extended to frequencies far above cutoff. J. Acoust. Soc. Am. 62:346–353.
Sigelmann, R.A., and J.M. Reid. 1973. Analysis and measurement of ultrasound backscattering from an ensemble of scatterers excited by sine-wave bursts. J. Acoust. Soc. Am. 53:1351–1355.
Welch, R., T.R. Jordan, and A.W. Thomas. 1984. A photogrammetric technique for measuring soil erosion. J. Soil Water Conserv. 39: 191–194.